INSTRUMENTAL CHARACTERIZATION OF MONTMORILLONITE CLAYS BY X-RAY FLUORESCENCE SPECTROSCOPY, FOURIER TRANSFORM INFRARED SPECTROSCOPY, X-RAY DIFFRACTION AND UV/VISIBLE SPECTROPHOTOMETRY

H. Wanyika, E. Maina, A. Gachanja and D. Marika
Department of Chemistry, School of Pure and Applied Sciences, Jomo Kenyatta University of Agriculture and Technology, Nairobi, Kenya
Email: e.maina40@yahoo.com

Abstract
Montmorillonite (MMT) clay has properties that would find applications in biotechnological and biomedical fields. In this study, naturally occurring MMT clay was purified using sedimentation and centrifugation techniques. Characterization of the prepared materials was done using X-ray Florescence (XRF), Fourier Transform-Infrared Spectroscopy (FT-IR Spectroscopy), UV-Visible Spectrophotometry (UV/VIS Spec) and X-ray Diffraction Spectrometry (XRD). XRF showed chemical composition of clay containing Fe_2O_3 as a major component. The structural composition as revealed using FT-IR, confirmed presence of various functional groups of Si-O, Al-OH and Si-O-Al as the major constituents. UV/VIS Spec confirmed presence of chromophores which absorbed light in the range of 270-300 nm confirming FT-IR results. XRD diffraction patterns confirmed presence of MMT clay as a major component with illite clay mineral existing as impurity. The sample contained good quality MMT clay and this study further confirmed the usefulness of spectroscopic techniques in determination of crystalline nature of montmorillonite clay.

Key words: Characterization, XRF; FT-IR, UV/VIS Spec; XRD, MMT clay

1.0 Introduction

Clay materials are abundant in most continents of the world and are familiar due to their low cost, high sorption properties, ion exchange and good adsorbent (Gupta *et al*., 2013). These clay materials are characterized by their layered structures which results to different classes of clays such as smectities (montmorillonite), Mica (illite), kaolinite, serpentine, vermiculite and sepiolite. Montmorillonite clay has two silica-oxygen tetrahedral sheets sandwiching and aluminum or magnesium octahedral sheets (Figure 1) (Wanyika, 2014). Magnesium or aluminium ions are octahedrally co-ordinated to six oxygen or hydroxyls. The replacement of silicon by aluminium in the tetrahedral layer makes the layers to be negatively charged. This results to cations like Na^+, K^+ and Ca^{2+} and Mg^{2+} to getting attracted to the layer surfaces to neutralize the negative charges (El-Messabeb-Ouali *et al*., 2013).

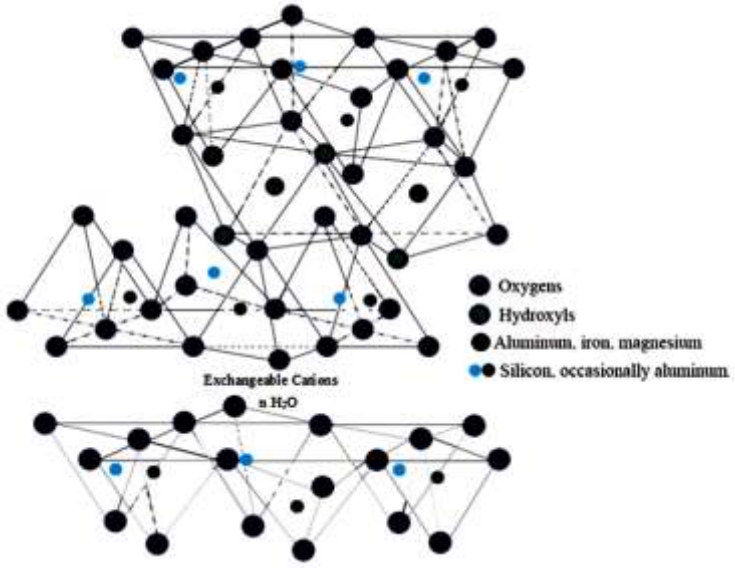

Figure 1: The structure of montmorillonite clay (Ismadji et al., 2015)

Fourier Transform Infrared Spectroscopy (FT-IR Spectroscopy) is an analytical tool which mainly compliments X-ray Diffraction (XRD) analytical technique in investigating clays and its minerals. FT-IR gives information about the mineral structure, isomorphic substituent's nature and distinct molecular water from constitutional hydroxyls. For instance, in clays, the OH stretching vibrations of structural hydroxyl groups is observed at 3626 cm^{-1}, Si-O stretching of cristobalite at 1067 cm^{-1}, AlAlOH stretching at 918 cm^{-1} and Al-O-Si deformation at 529 cm^{-1}. This technique is very common, economical and the clay spectra are obtained in a short period (Majedove, 2003). The peaks of resultant spectrum are analyzed and compared with the published literature thus helping in the identification of the exchangeable cations present in clay. X-ray Diffraction (XRD) is one of the most powerful characterization tool used for identifying crystalline minerals present in clay as it offers information about the basal spacing, texture and structural geometry on clay and thus is a technique basically used for mineral analysis (Ravisankar *et al*., 2010). XRD technique distinguishes the different types of clays deriving information about their structure composition and is thus the best analytical method as it is accurate, inexpensive, reliable, rapid and non-destructive (Oumabady *et al*., 2014).

2.0 Materials and Method

2.1 Solvents and Reagents

Solvents and reagents used throughout this research project were of analytical grade. Hydrochloric acid (analar) and absolute ethanol (analar) were purchased from Sigma-Aldrich, U.K.

2.2 Clay Sampling

Four composite clay samples denoted A, B, C and D were collected from Jomo Kenyatta University of Agriculture and Technology (J.K.U.A.T), Nairobi, Kenya from four different locations; farm, piggery, outside swimming pool and J.K.U.A.T. main gate areas respectively (Figure 2). The vegetation was first cleared using a knife and the top soil which was expected to contain organic matter was removed to about 20 cm. Samples (20 kg) were collected through digging 20 cm deep holes, they were sieved through 2 mm mesh size, put in plastic paper bags, carried to the laboratory and kept at 25 ± 2^{o} C for further analysis.

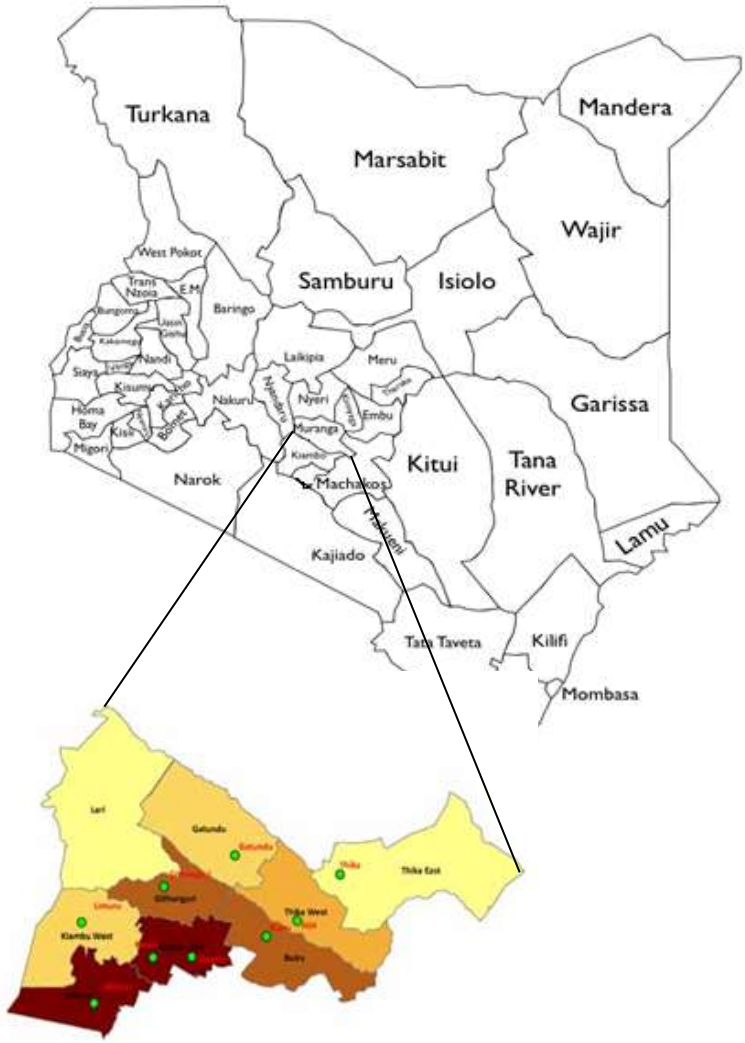

Figure 2: Sample collection area

The clay samples were purified using methods described by (James *et al*., 2008). In summary, the following method was followed; the sample was broken into smaller

lumps and larger particles consisting of pebbles, leaves and roots removed. Coarse particles and stones were removed by sieving through 2 mm mesh size. The resultant clay sample was then dried in an oven model no. 01410.CI about 150^{o} C to remove moisture and volatile organics. The sample was milled and passed through 420 µm mesh size. One part of the resultant milled sample was purified further by dispersing 100 g in 1 L of 10 % hydrogen peroxide in order to remove any soil organic matter present. The suspension was stirred and allowed to stand for 3 hrs. The clear suspension was decanted and the remaining clay was re-suspended in 1 L 0.5 M sodium hydroxide with stirring at 100 rpm for 45 minutes using a magnetic stirrer. The resulting solution was left to dry at 105^{o}C in the oven for 24 hrs.

2.2 Isolation of Clays

Clay particles were isolated from the purified clay using the following procedure: A sample (100 g) was dissolved in 1 L of distilled water. The solution was stirred using a magnetic stirrer for 4 hrs and left to stand for 12 hrs. The supernatant was pipetted out and centrifuged at 6000 rpm for 20 minutes to obtain the ≤ 2 µm particle sizes. The sediment was scooped out using a spatula, dried in the oven at 105^{o} C for 3 hrs and crushed into smaller particles using motor and pestle. The sample was allowed to pass through 200 µm mesh size.

2.3 Characterization of the Clays

2.3.1 Elemental Analysis using Total X-ray Fluorescence Spectrometry

The Fe, Mg, Ca, K and Mn contents of the clay samples were determined using S2 PICOFOX TXRF Spectrometer. The samples were prepared by digestion method which entailed weighing 1.00 g of the clay sample and transferring it into 250 mL conical flask, 10 mL of 1:1 HNO_3 was added, mixed and the slurry covered with a watch glass. The mixture was heated to 90^{o} C and refluxed for 15 minutes without boiling. It was then cooled and 5 mL of concentrated HNO_3 was added, covered and refluxed for 30 minutes. Brown fumes were generated, which indicated oxidation of the clay sample by HNO_3. The step of addition of 5 mL of concentrated HNO_3 was repeated until no further brown fumes were given off indicating complete reaction.

The glass bottles that were used in the experiment were first cleaned by immersing them in 1.5 % concentrated HNO_3 solution overnight and rinsed with dilute nitric acid solution. The rinsing solutions were analyzed for any trace impurity and no impurities were found. The clay sample solutions were subjected to TXRF to analyze the chemical composition or elements present. The quartz sample support were also cleaned with 1.5 % concentrated HNO_3 and checked for contamination by acquiring the TXRF spectrum before the sample deposition by measuring the TXRF spectrum. All sample standards were diluted with 1.5 % concentrated HNO_3. Clay sample solutions (5 mL) were taken separately into the earlier cleaned glass bottles. Ga internal standard solution (50 µl of 5 µg/ mL) was

mixed with 5 mL of clay sample solutions. Aliquots (20 µl) were deposited ten times independently on six quartz sample supports so that 200 µl of the clay sample solutions were deposited and dried on IR lamp. The TXRF spectrum for each sample was recorded for 20 minutes.

2.3.2 Determination of Basal Spacing and Crystallite Size

The clays were subjected to further purification following the method of (Ray, 2007). In summary, the following procedures were followed: Iron Oxide Impurities were removed by treating clay (50 g) with sodium citrate reagent made by dissolving 15.06 g of sodium citrate in 200 mL of distilled water followed by addition of 1.50 g of $NaHCO_3$ and 14 g of NaCl. The mixture was heated to 80^{o} C for 30 minutes. Then, the solution was centrifuged at 600 rpm for 20 minutes and the supernatant discarded. Lastly, the nano clay was washed three times with 1 M NaCl. Carbonate impurities were removed by suspending the clay sample from the previous procedure in 1 L aqueous solution containing 136 g sodium acetate at pH 4.8 followed by washing thrice with 1 M NaCl. In order to remove organic matter, the dry clay sample was re-suspended in 30 % H_2O_2 and heated to 80^{o} C for 30 minutes. The suspension was centrifuged at 600 rpm for 20 minutes. Excess H_2O_2 was removed by washing the sample three times with distilled water followed by centrifugation at 6000 rpm for 20 minutes and oven drying at 105^{o} C.

Finally, a part of the sample was treated by exposure to vapour of ethylene glycol and dried at 60^{o} C in the oven (Lab Manual, 2008) while the other part was heated in the oven at a temperature of 550^{o} C for 40 minutes in order to collapse any expandable layers (Moore and Reynolds, 1989). The treated samples were analyzed by X-ray Diffractometer as described by (Guegan *et al*., 2009). The X-ray diffractometer measurements were done with Cu-Kα radiation of wavelength 1.5418A^{O}on Rigaku Manniflex II Desktop operating at 40Kv and 30mA. The scan range was 1^{o} through 45^{o} at a scanning rate of 1^{o}/ min with a step size of 0.04^{o}. Diffraction peaks of the raw clay sample were compared with those of standard clay materials. The sample crystallite size of the clay was measured using Debye-Scherer's equation from the XRD peaks expressed as equation 1:

$$D = K\{\frac{\lambda}{(^{\beta}COS\Theta)}\} \quad \text{.....Equation (1)}$$

Where D = Crystallite size, K = 0.89 (constant), λ = X-ray wavelength 1.540562 (Å), $^{\beta}$ = full width at half maximum, Θ = scattering angle (Hassani *et al*., 2015).

2.3.3 Determination of Cation Exchange Capacity (CEC) of Clay

The CEC of clay was determined using Ammonium Acetate method (Mehlich, 1938). The standard solutions of the exchangeable cations; K^{+}, Na^{+}, Ca^{2+} and Mg^{2+} were first prepared as described: Potassium, Sodium, Calcium and Magnesium Standard Solutions of 100 ppm were prepared in triplicates by dissolving 0.01 g each of K_2SO_4 and NaOH, 0.06 g of $Ca(NO_3)_2$ and 0.04 g of $MgSO_4$ in 100 mL of distilled water.

Serial dilutions in the range of 0.1-1.5 ppm for Potassium and Sodium, 0.15-5 ppm for calcium and 0.1-1.5 ppm for Magnesium were made in triplicates. In all the standards, about 1 mL of the 5 % La_2O_3 solution was added and solution shaken for 15 minutes. Lanthanum oxide solution (5 %) was prepared by dissolving 50 g La_2O_3 in 100 mL concentrated HCl, the mixture was cooled and diluted to 1 L with distilled water. Atomic absorption spectrophotometer (AAS), model no. 210VGP with hollow cathode lamp fitted with specific element being analyzed and slight adjustment on its respective wavelength. Calibration mode was linear and signal measurements were done with peak area (Njoka *et al*., 2015), was used to measure standards and sample absorbance for Magnesium and Calcium .FES model no. AFP 100 was used for Potassium and Sodium. The concentrations of the respective cations in the different samples were determined using regression equations of best lines of fit.

Ammonium Acetate (1 M, pH 7) was prepared by adding 57 mL of glacial acetic acid and 68 mL of concentrated Ammonium Hydroxide to 800 mL of distilled water in a 1 L volumetric flask. The solution was allowed to cool, pH adjusted to 7.0 using 3 M acetic acid and diluted to 1 L mark using distilled water. Each clay sample (2.5 g) was put in 250 mL beaker and 25 mL Ammonium Acetate solution added. The solution was shaken for 30 minutes and was then filtered through a whatman filter paper no. 1. Each clay sample solution (100 µL) was pipetted and transferred to 50 mL volumetric flask. La_2O_3 (2 mL of 5 %) solution was added and made to mark with distilled water. The samples were analyzed for K^+ & Na^+ using FES and Mg^{2+}& Ca^{2+} using AAS.CEC calculations were done using equation (2):

$$Y^{n+}\ (\text{meq}/100\text{gms}) = \frac{\frac{\text{mg}}{\text{ML}}\text{y x d.f}}{eq.\ weight of y} \quad \text{.....Equation (2)}$$

where y is the element of interest and n=1 or 2.

2.3.4 Functional Groups Determination Using Fourier Transform-Infrared Spectroscopy (FT-IR Spectroscopy)

The samples were run using SHIMADZU FT-IR spectrophotometer model no.8400 in the range of 400 – 4000cm^{-1} and the sample was scanned 20 times. The sample was prepared as a KBr disc by mixing 0.01mg of air dried clay with 0.25 mg dried potassium bromide (KBr).

2.3.5 UV-Visible Spectrophotometry

About 1.00 g of the clay sample was mixed with 10 mL of concentrated nitric acid and was refluxed at 90^o C for 15 minutes. Additional 5 mL portions of concentrated nitric acid were added to the cooled sample and refluxed at 95^o C for 30 minutes until more addition did not produce brown fumes. The solution was then refluxed for 2 hrs. Once the solution was cooled to room temperature, 2 mL distilled water and 3 mL of 30 % H_2O_2 were added and the solution warmed until effervescence ceased. Additional 1 mL portions of hydrogen peroxide were added followed by heating until effervescence became negligible. The solution was then refluxed for

30 minutes and allowed to cool. Concentrated HCl (10 mL) was added followed by 15 minutes of refluxing. After the solutions cooled, it was filtered through Whatman filter paper no.1 into 100 mL volumetric flask and was brought to volume with distilled water.

The sample solution was diluted in the ratio 1:50 (v/v) portions of sample into distilled water respectively. One of the cuvettes was filled with distilled water and the other was filled with the diluted sample solution. The sample was then run in the SHIMADZU UV-Visible Spectrophotometer model no. 1800 with the scan range of 200-700 nm and results were analyzed.

3.0 Results and Discussion

3.1 Sample Collection and Purification

3.1 Purification of Clays

The clay soil samples were collected from J.K.U.A.T farm from four different sites and denoted as A, B, C and D. On sieving through 2.0 mm mesh size, clay samples A and B yields was high (Figure 3). This may be due to the sample location contributed to ploughing factors. Sample D had the lowest yield due to less agricultural activities in the area. On chemical purification stage, there was high rate of effervescence, emission of heat and gasses and this method proofed to be more effective in the removal of inorganic matter. The percentage clay yield of these samples increased due absorption of water. The process of isolation of ≤ 2 µm clays had the smallest quantity yield. This was due to sample collection from the supernatant.

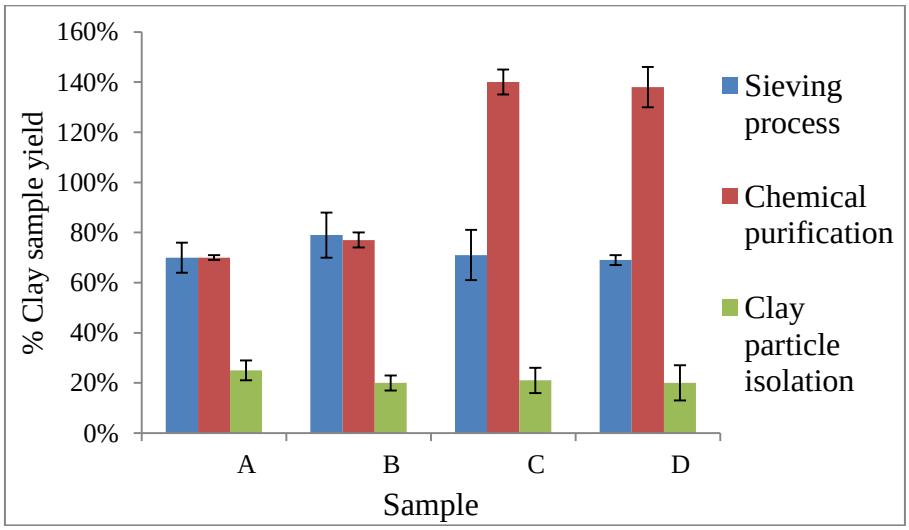

Figure 3: Different clay sample purification methods

3.3 Characterization of the Clays

3.3.1 Elemental Composition

TXRF results collected showed presence of major and minor elements (Figure 6). Iron (Fe) was the major element which occurred in the range of 30-54 % when expressed as Fe_2O_3 (table 2), while all other elements; K, Ca, Cu, As, Pb, Sr, Mn and Rb occurred as minor elements (table 2) (Antoaneta *et al*., 2009). According to Muriithi *et al*., (2012), montmorillonite clays minerals have complex structures of Fe^{2+}, Fe^{3+} and Mn^{2+} ions in octahedral sheets embedded with other metal cations like Si^{4+} and Al^{3+} in the tetrahedral layer. This highest Fe_2O_3 percentage in the clay samples signified presence of montmorillonite clay minerals. Potassium and calcium ions occurred in the clay gallery spaces while the other minor elements were embedded in clay structure.

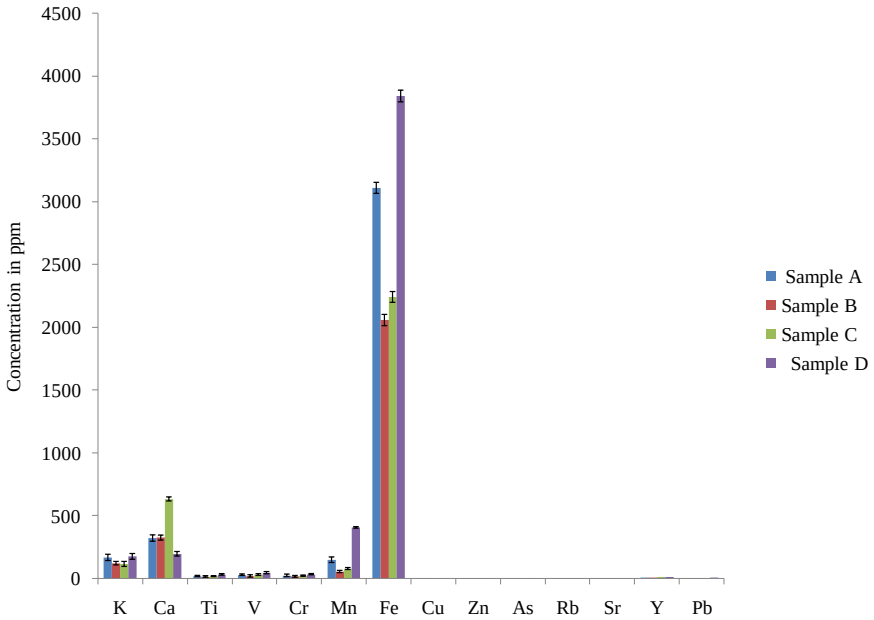

Figure 4: Elemental composition (ppm) of different clay samples

Table 1: Oxide levels (%) of the clay samples

	A	B	C	D
Fe_2O_3	44.00	30.00	31.00	54.00
CaO	4.10	4.10	7.00	2.40
K_2O	2.40	2.40	2.40	2.40
MnO	3.10	2.00	1.00	1.00

3.3.2 FT-IR Spectra

After the samples were subjected to FT-IR spectroscopy determination, the spectra were found to be similar in all the samples (Figure 5). The Si-O and Al-OH were the main functional groups observed in the range of 1000 cm^{-1} and 500 cm^{-1}. Intensive peaks at 528.5 $cm^{-1}$was due to the bending vibrations of Al-O-Si bond (Navratilova et al., 2007) while bands at 914-916 cm^{-1} corresponded to the Al-OH bending vibrations. The doublet at 780-798 cm^{-1} was due to Si-O-Si inter tetrahedral bridging bonds in SiO_2 and OH deformation bond of gibbsite (Saiki and Parthasarathy, 2014). Si-O stretching vibrations were observed at around 780-686 cm^{-1} showed presence of quartz (Thambavani and Kavitha). Strong bands at around 3620 cm^{-1} showed presence of hydroxyl linkage while broad band at 450 cm^{-1} and bands at 1650-1641 cm^{-1} in the clay spectrum indicated possibility of water of hydration or H-O-H bending of water in the adsorbent due to the hydrous nature of the clay materials (Nayak and Singh, 2007). The chemical composition of this clay mineral is clearly indicated by the position of the band (Patel *et al*., 2006). The results were helpful in identification of the various forms of minerals present in clay. According to Adikary and Wanasinghe (2012), the important bands that are needed for identification of montmorillonite clay is at absorption bands at position 1, 2, 7 and 8 (Table 2).

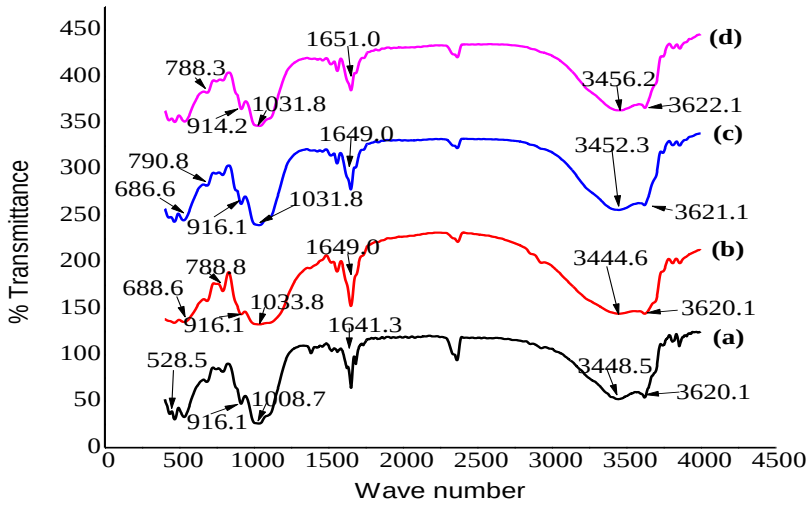

Figure 5: FT-IR spectra of; (a) Clay A, (b) Clay B, (c) Clay C and (d) Clay D

Table 2: FT-IR absorption bands of different clay samples

Absorption band position	Theoretical Montmorillonite	Sample Wave numbers (cm^{-1}) A	B	C	D	Assignments
1	3630	3620.1	3620.1	3620.1	3622.1	Al/Mg--O-H stretching (Inter-octahedral)
2	3427	3448.5	3444.6	3452.3	3456.2	H-O-H stretching of structural hydroxyl groups & water
3	1636	1641.3	1649.0	1649.0	1651.0	OH deformation of water
4	_	1558.4	1558.4	1558.4	1558.4	C-N stretching
5	_	1514.0	1519.8	1515.9	1508.2	Aromatic nitrate
6	1065	-	-	-	-	Si-O stretching of quartz in plane vibration
7	1049	1008.7	1033.8	1031.8	1031.8	Si-O stretching
8	918	916.1	916.1	916.1	914.2	Al-Al-OH bending/ deformation
9	-	788.8	790.8	788.8	788.8	Si-O quartz
10	695	_	686.6	686.6	688.5	AlAlOH bending

3.3.3 UV-Visible Spectrophotometry

The spectra of the UV-Visible sample analysis are shown in Figure 6 with the peaks ranging from 200-300 nm. This proved presence of conjugated systems as earlier observed using FT-IR technique (Cuhna *et al*., 2009). In sample A, B and C, the characteristic bands present at 288 and 236 nm were attributed to $\pi \rightarrow \pi^*$ transition of Si=O functional group. Absorption band at 298.50 nm and 290.50 nm in samples A and D respectively were attributed to $n \rightarrow \pi^*$ transitions due to presence of lone pairs of electrons on hydroxyl substituent and Si-O-Si.

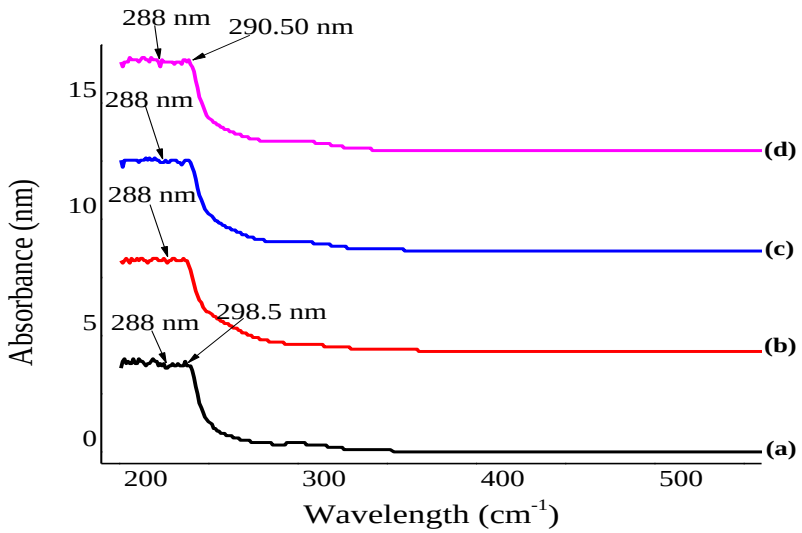

Figure 6: UV-Visible Spectra of: (a) Clay A, (b) Clay B, (c) Clay C and (d) Clay D

3.3.4 XRD Analysis

XRD was used for qualitative evaluation of the purified clay samples and the d-values were compared with those published in literature. The identification of the clay minerals was accomplished by careful consideration of peak position and intensities in comparison with the spectra from Selected Powder Diffraction Data for Minerals and Powder Diffraction File Search Manual Minerals. The analysis was measured in the range of 1-45^{o} 2θ and the diffraction patterns were obtained at different clay treatment; (**a**) Ethylene glycol (EG) and (**b**) at high temperatures of 550^{o}C (Figure 7). The results revealed characteristics of montmorillonite clay mineral due to diffraction peaks at d-spacing 16.0136Å and 3.0214Å at 7.94^{o}2Θ and at 28.95^{o} 2Θ respectively (Lugwisha, 2011). On heating the diffraction peaks shifted to 9.6849 Å and 3.2283Å respectively due to phase transformation (Alluminium-hydroxy-montmorillonite to stable oxy-alluminium-montmorillonite (Navratilova *et al*., 2007). The diffraction peaks occurring at 16.09^{o} 2Θ and 27.61^{o} 2Θ and corresponding to d-spacing of 4.8424Å and 3.2283Å respectively appeared on heating due to presence of illite in the sample as an impurity. Njoka *et al*., (2015), suggested that strongest reflection resulting to an intense peak observed at 16.0136Å, at 7.94, 2Θ, indicates greater quantity of MMT clay mineral in comparison to illite in the sample.

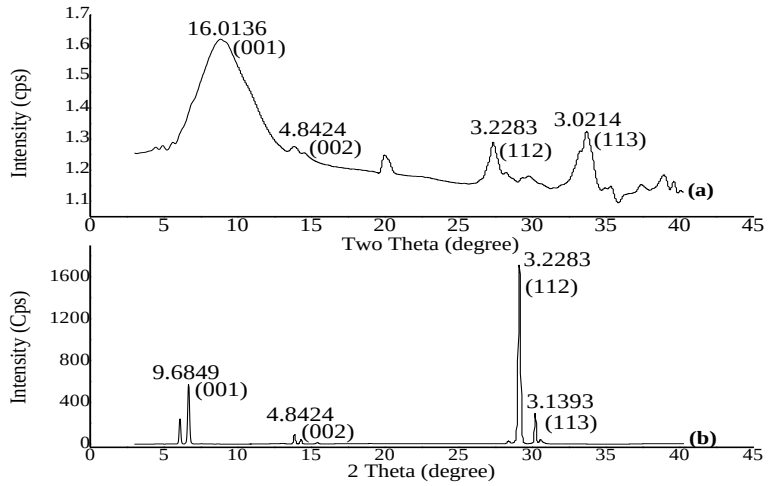

Figure 7: X-ray diffraction patterns of unmodified clay minerals at different sample treatment; (a) treated with Ethylene Glycol and (b) heated at high temperatures of 550^{o} C

3.3.5 Crystallite Size

The sample diffraction peaks in sample (b) had sharp peaks indicating good crystallinity of the sample on treatment with temperatures of 550^{o} C (Bindu and Sabu, 2014). This indicated that high temperatures acted as a driving force for the growth of the crystallite size. These temperatures can thus be used as crystallite activation energy as observed in Figure 7. Similar results were observed by Monshi *et al*., (2012). This could be as a result of removal of water and hydroxyl groups present in clay (Gaber *at al*., 2013).

3.3.6 Cation Exchange Capacity (CEC) of the Clays

Ammonium acetate method for Cation Exchange Capacity (CEC) determination was settled on for classification of the soil purposes. According to Aprile, (2012), the most important exchangeable cations in the soil are calcium (Ca^{2+}), magnesium (Mg^{2+}), sodium (Na^{+}) and potassium (K^{+}). Respective calibration curves were drawn for the four ions under consideration (Figure 8). The square of the product moment correlation coefficient (R^2) values ranged between 0.993 for K^{+} and 0.999 for Ca^{2+} standards which indicated linearity of the calibration graph. The CEC of individual ions and the total thereof is indicated in (Table 3). In all the samples, CEC of Na^{+} ions in the clay gallery spaces was the highest meaning that the clay exchange sites contains mostly sodium ions followed by Mg^{2+} and K^{+} while that of Ca^{2+} had the lowest quantity. High CEC in soils A, C and D depended on mineralogical composition of the soil sample. High CEC values of more than 75 meq/ 100 gms indicates soil content with more than 80 % montmorillonite clay

present (Jaqueline *et al*. 2013) and this indicated without doubt that soil A, C and D was montmorillonite clay as earlier indicated by FT-IR and XRD techniques. The difference in CEC values of the soils A, C and D may have been as a result of the amount of organic matter present which contributed to higher CEC values

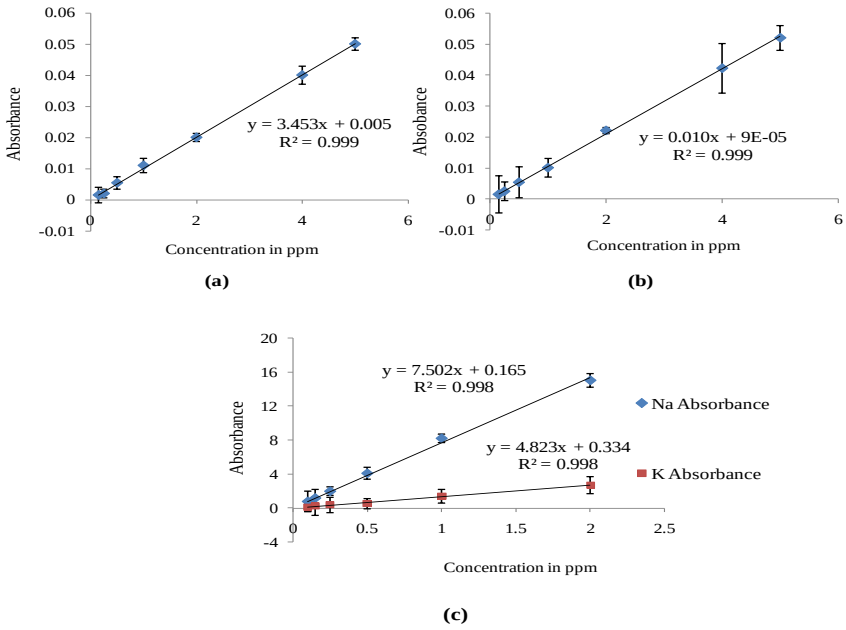

Figure 8: Calibration curves for; (a) Mg^{2+} (b) Ca^{2+} and (c) Na^{+} and K^{+}

Table 3: Total CEC of the different cations

Cation Exchange Capacity meq/ 100 gms					
Sample	Ca^{2+}	Mg^{2+}	Na^{+}	K^{+}	Total CEC
A	0.003	4.6817	81.22	6.504	92.4087±0.2
B	0.0003	0.7892	65.64	2.602	69.0315±0.4
C	0.0035	4.1033	82.55	4.5527	91.2095±0.2
D	0.0009	5.3667	83.212	3.2519	91.8315 ±0.1

4.0 Conclusions

The chemical analysis of MMT clay using XRF showed to consist of Iron Oxide, alumina and silica as major constituents while Calcium, Magnesium and Potassium exist as minor constituents. Ethylene glycol and heat treatments were useful in MMT clay identification using XRD analysis. The existence of the named minerals was further confirmed using FT-IR technique.

Acknowledgements
This work was supported by National Commission for Science, Technology and Innovation (Innovation Grant 2014/2015 FY), Nairobi, Kenya.
Conflict of Interests: The authors declare that there is no conflict of interests regarding the publication of this paper.

References

Adikary, S. and Wanasinghe. D. (2012). Characterization of locally available montmorillonite clay using FTIR technique. University of Moratuwa, Chemistry Department, Hong Kong, pp.1-6.

Antoaneta, E., Alina, B. and Georgescu, L. (2009). Determination of heavy metals in soils using XRF technique. Journal of Applied Physics , 55, pp.815-820.

Bindu, W. and Sabu, E. (2014). Estimation of lattice strain in ZnO nanoparticles: X-ray peak profile analysis. Journal of Theoritical Applied Physics , 8, 123-134.

Cuhna, T., Novotny, E., Madari, B., Martin, L., Rezende, L. and Benites, V. (2009). Spectroscopy characterization of humic acids isolated from Amazonian Dark Earth soils. Springer Science , 5, pp.363-372.

El-Messabeb-Ouali, A., Benna-Zayani, M., Ayadi-Trabelsi, M., Sauvé, M., and Sauve, S. (2013). Morphology, structure, themal stability, XR-Diffraction and infrared study of hexadecyltrimethylammonium bromide-modified smectite. International Journal of Chemistry , 5, pp.12-28

Gaber, A., Abdel-Rahim, A., Abdel-Latief, Y. and Abdel-Salam, N. (2013). Influence of calcinations temperature on the structure and porosity of nanocrystalline SnO2 synthesized by conventional precipitation method. International Journal of Electrochemical Science , 9, pp.81-95.

Guegan, R., Gautier, M., Beny, J. and Muller, F. (2009). Adsorption of a C10E3 non-ionic surfactant on a Ca-Smectite. Clay and clay minerals 57: pp.502-509.

Gupta, A., Amitabh, V., Kumari, B., Mishra, B. (2013). FTIR and XRPD studies for the mineralogical composition of Jharkhand bentonite. Research Journal of Pharmaceutical, Biological and Chemical Sciences , 4, pp.360-369.

Hassani, A., Khataee, A., Karaca, S. and Shirzad-Siboni, M. (2015). Surfactant-modified montmorillonite as a nanosized adsorbent for removal of an insecticide: Kinetic and isotherm studies. Journal of Environmental Technology 10: pp.1-42

Ismadji, S., Soetaredjo, F. and Ayucitra, A. (2015). Natural clay minerals as environmental cleaning agents. Journal of Clay Materials for Environmental Remedation , 8, pp.5-37.

James, O., Adediran, M., Adekola, F., Odebumni, E and Adekeye, J. (2008). Benefication and characterization of a bentonite from north-eastern Nigerian. Journal of North Carolina Academy of Science , 124, pp.154-158.

Jaqueline, A., Calabria, A., Daniela, N., Ana, C., Ladeira, Q, Stela, D. and Talita, S. (2013). Determination of the cation exchange capacity of the bentonite exposed to the hyperalkaline fluid. International Nuclear Alantic Conference.

Lab Manual. (2008). GeoEnvironmental Research Group.

Lugwisha. A. (2011). Identification of clay minerals of the Eastern Southern region of Lake Victoria by ethylene glycol and heat: x-ray diffraction and infrared spectroscopy studies. Tanzanian Journal of Science , 37, pp.167-178.

Majedove, J. (2003). FTIR techniques in clay minerals studies. Journal of Analytical Chemistry , 25, pp.1169-1174.

Mehlich, A. (1938). Use of triethanolamine acetate-barium hydroxide buffer for the determination of some base properties and lime requirements of soil. Journal of Soil Science Society , 29, pp.374-378.

Moore, D and Reynolds, R. (1989). X-ray diffraction and the identification and analysis of clay minerals. Oxford University, Oxford.

Muriithi, N., Karoki, K. and Gacanja, A. (2012). Chemical and mineral analyses of Mwea clays. International Journal of Physical Science , 44, pp.5865-5869.

Navratilova, Z., Wojtowicz, P., Vaculikova, L. and Sugarkova, V. (2007). Sorption of alkylammoium cations on montmorillonite. Journal of Acta Geodynamica Geomaterialia 4: pp.59-65.

Nayak, S. and Singh, K. (2007). Instrumental characterization of clay by XRF, XRD and FTIR. Journal of Bulletin of Material Science 30: pp.235-238.

Njoka, E., Ombaka, O., Gicumbi, J., Kibaara, D. and Nderi, O. (2015). Characterization of clays from Tharaka-Nithi county in Kenya for industrial and agricultural applications. African Journal of Environmental Science & Technology , 9, pp.228-243.

Oumabady, A. Rajendran, M. and Selvaraju, R. (2014). Mineralogical identification on polluted soils using XRD method. Journal of Environmental Nanotechnology , 3, pp.22-29.

Patel, H., Rajesh, S., Hari, B. and Raksh, J. (2006). Clays for polymer nanocomposites, paints, inks, greases and cosmetics formulations, drug delivery vehicle and waste water treatment. Indian Academy of Sciences , 29, pp.133-145.

Preeti, S. and Singh, B. (2007). Instrumental characterization of clay by XRF, XRD and FTIR. Journal of Academy Sciences , 30, pp.235-238.

Ravisankar, R., Senthilkumar, G., Kiruba, S., Chandrasekaran, A. and Prince, J. (2010). Mineral analysis of coast sediment samples of Tuna, Gujarat, India. Indian Journal of Science and Technology , 7, pp.1169-1174.

Ray, F., Yunfei, X. and Hongping, H. (2007). Modification of the surfaces of Wyoming montmorillonite by the cationic surfactants alkyl trimethyl, dialkyl dimethyl and trialkyl methyl ammonium bromides. Journal of Colloid and Interface Science 305:pp.150-158.

Saikia, B. and Parthasarathy, G. (2014). Fourier transform infrared spectroscopic characterization of kaolinite from assamad Meghalaya, northeastern India. Journal of Modern Physics 1: pp.206-210.

Thambavani, S. and Kavitha, B. (2014). Mineralogical characterization of river bed soil from Tamilnadu by FT-IR, XRD and SEM/EDAX. International Journal of Advanced Research 2: pp.656-659

Wanyika, H. (2014). Controlled release of agrochemicals intercalated into montmorillonite interlayer space. The Scientific World Journal , 10, pp.1-9.